Applied Surface Science 548 (2021) 149093

Contents lists available at ScienceDirect

Applied Surface Science

journal homepage: www.elsevier.com/locate/apsusc

Short Communication

Phosphate incorporation in anodic hafnium oxide memristors

Ivana Zrinski [a], Cezarina Cela Mardare [a], Luiza-Izabela Jinga [b], Jan Philipp Kollender [a,c], Gabriel Socol [b], Achim Walter Hassel [a], Andrei Ionut Mardare [a,*]

[a] Institute of Chemical Technology of Inorganic Materials, Johannes Kepler University Linz, Altenberger Str. 69, 4040 Linz, Austria
[b] National Institute for Lasers, Plasma and Radiation Physics, Atomistilor Str. 409, 077125 Bucharest-Magurele, Romania
[c] EMPA, Laboratory for Joining Technologies & Corrosion, Swiss Federal Laboratories for Materials Science and Technology, Überlandstrasse 129, 8600 Dübendorf, Switzerland

ARTICLE INFO

Keywords:
Memristor
Anodization
Hafnium oxide
Phosphate buffer electrolyte

ABSTRACT

The electrochemical fabrication of memristive devices based on Hf is demonstrated. Electrolyte incorporation in memristors is confirmed in oxides grown in 0.1, 0.5 and 1 M phosphate buffers. The impact of phosphate species on conductive filaments formation is described. The use of 1 M phosphate buffer allows formation of Hf-O-P compounds that hinder phosphate incorporation into the bulk of the memristors. Endurance, retention and memory characteristics of anodic Hf memristors suggest improved properties, as compared with previous reports, especially after mild heat treatments of devices. High resolution atomic imaging of conducting filaments allowed further understanding of memristive switching in HfO_2.

1. Introduction

Memristive characteristics in a metal-insulator-metal (MIM) structure were firstly reported at Pt/TiO_2 interface [1]. An applied electric field moves the positively charged oxygen vacancies inside an oxide layer sandwiched between two electrodes. Enormous scientific effort is put in investigation of conductive filaments (CF) formation based on local redox reactions within the oxide [2,3]. The CF deletion or formation allows switching between low and high conductance states (OFF and ON, respectively), thus defining the operational memory of the memristive device. Apart from predominantly vacuum-based fabrication approaches [4,5], new generations of non-volatile memory systems based on anodic oxides on valve metals recently emerged [6–10]. These anodic memristors make use of an inexpensive fabrication route involving electrical field driven oxide growth from a parent metal in contact with a liquid electrolyte [11], with accurate nm thickness control [9]. They have low power consumption and capabilities of high density data storage and high data endurance and retention for resistive random access memories (ReRAMs), neuromorphic computing and sensing applications [12–14].

Anodic oxidation allows direct oxide growth control *via* electrochemical parameters and their manipulation ensure high-quality films [15,16]. The replacement of common and often expensive fabrication methods for memristive applications (i.e. sputtering [17–19], pulsed laser deposition [20,21], atomic layer deposition [22,23] and various chemical methods) with the anodization approach is extremely relevant. This is due to overall costs reduction in industrial implementation and shorter turnover time, required when designing novel materials [24]. Tantalum and Ti anodic oxides were reported as noteworthy solid electrolytes for memristive switching. However, the use of anodic HfO_2 has been debated only once together with Nb [25]. The HfO_2 is already used as high dielectric constant material in capacitors or as gate oxide for transistors in modern electronics [26,27]. The MIM structures necessary for memristive devices are identical to those used for capacitor applications, thus the know-how and driving force toward applications of HfO_2 already exist. Anodization of Hf allows formation of an intimate interface between the parent metal and its own oxide, eliminating device issues related to interfacially trapped defects or impurities. Thus, apart from decreasing device fabrication costs, the use of anodic HfO_2 is expected to improve memristor stability, lifetime and electrical fatigue. Additionally, oxide exposure to a liquid electrolyte during anodization may be beneficial to the memristive switching due to the additional surface chemistry, otherwise absent when vacuum technology is used for HfO_2 deposition.

In this letter, incorporation of electrolyte species in HfO_2 memristors during anodization process in neutral phosphate buffers (PB) is demonstrated for the first time. Apart from all chemical advantages of PB (i.e. nontoxic, easy disposable, low costs components, minimal pH

* Corresponding author.
E-mail address: andrei.mardare@jku.at (A.I. Mardare).

https://doi.org/10.1016/j.apsusc.2021.149093
Received 14 December 2020; Received in revised form 15 January 2021; Accepted 17 January 2021
Available online 2 February 2021
0169-4332/© 2021 The Author(s). Published by Elsevier B.V. This is an open access article under the CC BY license (http://creativecommons.org/licenses/by/4.0/).

change with temperature), electrolyte species incorporated in the insulating oxide layer improved electrical characteristics of memristive devices.

2. Experimental

Metallic Hf thin films, 300 nm thick, were deposited by sputtering (Mantis Deposition, United Kingdom) on thermally oxidized Si wafers (950 °C, 24 h). The base pressure of the sputtering vacuum system was in the range of 10^{-6} Pa. The deposition from a Hf target (99.95% Demaco, The Netherlands) was done at room temperature in Ar at $5 \cdot 10^{-1}$ Pa. The electrochemical anodization process of Hf films was carried out potentiodynamically in 0.1 M, 0.5 M and 1 M PB electrolyte using a potential scan rate of 100 mV s^{-1} up to 8 V (*vs.* the standard hydrogen electrode - SHE). The 1 M PB buffer was prepared following the standard recipe by mixing 1 M Na_2HPO_4 and 1 M NaH_2PO_4 solutions [28]. The buffer was diluted in order to prepare 0.5 M and 0.1 M PB electrolytes using ultrapure water (Millipore). The pH of all solutions was adjusted to 7.0. All the chemicals were of analytical grade (Merck, Germany). A CompactStat potentiostat (Ivium Technologies, The Netherlands) was responsible for Hf anodization using a graphite foil as counter electrode and Hg/Hg_2SO_4/sat. K_2SO_4 electrode (0 V *vs.* $Hg/Hg_2SO_4 = 0.640$ V *vs.* SHE) as reference electrode. The anodic Hf memristor fabrication was completed by sputtering Pt top electrodes (200 μm in diameter, 100 nm thick) through a Ni shadow mask foil (30 μm thick, Mecachimique, France). The sputtering was completed in Ar atmosphere ($5 \cdot 10^{-1}$ Pa) at room temperature from a high purity target (99.95%, MaTeck, Germany).

Electrical and thermo-electrical measurements were performed on independent memristors with a Keithely 2450 source meter by contacting top and bottom electrodes. An electrical heater placed under the sample allowed temperature control. The Hf bottom electrode was biased whereas the Pt top electrodes were grounded. The formation of memristors is a critical factor for the proper memristive switching of the devices. Each memristor was formed by biasing the electrode in positive direction up to 5 V while limiting the current at low values in the nA-μA range for avoiding irreversible dielectric breakdown. Once successfully formed, the devices were switched in a voltage sweep cycle from 0 V to 5 V, 5 V to −5 V and −5 V to 0 V while constantly monitoring the current. Endurance and retention measurements were accomplished by biasing memristors directly at their switching voltages until their failure. The memristive device resistance was read at 0.02 V within 3.8 ms for both endurance measurements and retention of ON and OFF states.

High resolution transmission electron microscopy (TEM - JEOL JEM-2200FS) with an acceleration voltage of 200 kV was performed for visualizing conducting filaments. The superficial and in-depth chemical composition of memristors was analysed by energy dispersive X-ray spectroscopy (XPS - ESCALAB Xi+, Thermo SCIENTIFIC Surface Analysis) [29]. Depth profiles were obtained by Ar sputtering of a 2×2 mm^2 area at 2 keV ion energy.

3. Results and discussion

Representative cross-sectional TEM images of the memristive structure are presented in Fig. 1. Both metallic electrodes have thicknesses of approximately 300 nm, while the anodic oxide is about 17 nm thick. In Fig. 1a it can be seen that both electrodes are dense and a good adherence to the oxide is suggested by the lack of any visible defects. The small rectangular region emphasised in Fig. 1a is presented in Fig. 1b with atomic resolution. Both metallic electrodes show polycrystalline structures, and the Hf/HfO_2 interface appears smoother when compared to the Pt/HfO_2 interface. The smoother appearance of the Hf/HfO_2 interface is related to the growth dynamic of the anodic oxide directly from the Hf parent metal under high field conditions [30]. In the case of memristive oxides fabricated by deposition techniques (e.g. sputtering), deposition of HfO_2 will produce a much sharper interface with the bottom electrode (similar to the Pt/HfO_2 in Fig. 1b). This represents the fundamental difference between the present electrochemical fabrication route and other deposition techniques. In this study, each Hf atom forming oxide molecules originates from the Hf bottom electrode and their absolute position does not vary much since Hf^{4+} has a very low ionic transport number as compared to O^{2-} which is much more mobile [31]. As a result, the oxide is formed primarily at the metal/oxide interface by partly consuming the Hf electrode. Additionally, it was demonstrated before that thin anodic oxides grown on Hf are crystalline [32]. However, a careful observation of Fig. 1b also allows visualizing amorphous regions inside the anodic oxide by localized atomic disarray regions.

In previous studies, O vacancies and cations were reported to accumulate in trapezoidal shapes close to the top Pt electrode during the CF formation [33]. Fig. 1b shows two such regions (marked with red dotted lines) at the Pt interface and a partially formed CF is highlighted (between blue dotted lines). The alignment between one accumulation region and the CF indicates its growth dynamics. Randomly positioned accumulation regions are the starting point for the redox reactions leading to CF formation [3]. The redox process occurring during OFF/ON transition affects the crystallinity in the CF vicinity producing its disordered appearance. The size and position of CF may depend on the metal cations and, particularly in this work, on electrolyte species trapped inside during anodic formation. The anodic memristor

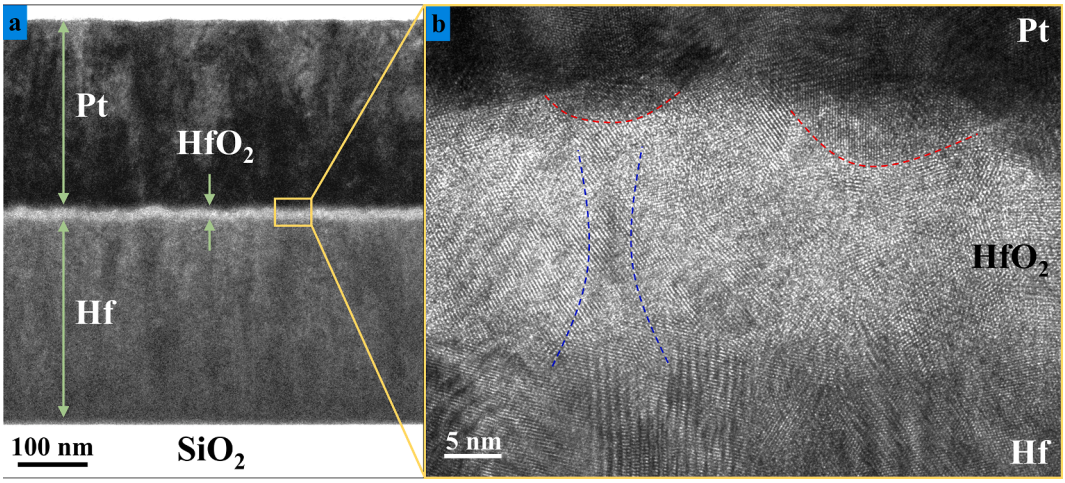

Fig. 1. TEM imaging of HfO_2 memristive devices: Cross section analysis indicating the thickness of the metallic electrodes in relation to the active oxide layer (a) and atomic resolution image visualizing a conducting filament and two accumulation zones responsible for the memristive effect (b).

illustrated in Fig. 1b was switched in OFF state before analysis, thus the CF is partially oxidized or deleted.

The chemical composition of oxides electrochemically grown in different dilutions of PB was studied by XPS and representative results are collected in Fig. 2. Generally, electrolyte incorporation in anodic oxides was reported [34,35] but its influence on memristive behaviour remains grossly unevaluated. Additionally, most of previous studies refer to much thicker oxides than requested for memristive applications according to modern devices power requirements. The electrochemical parameters used here were optimized for producing a thin and dense HfO_2 [36]. Control of chemical processes in various applications require the use of different buffers and their conductivity variability is noted [37]. An XPS surface survey is presented in Fig. 2b. For all analysed oxides, the presence of Hf and O was the most evident, but also P, C, Zr and Na peaks are always found for oxides formed in PB. The presence of P, C and Na is attributed to incorporation of phosphates during oxide growth. For clarifying this aspect, high resolution XPS of Na 1s and P 2p peaks (highlighted in the survey) are additionally presented in Fig. 2a and c, respectively. Deconvolution of both peaks allowed identification of NaH_2PO_4 and Na_2HPO_4 in all cases.

Depth profiles XPS were obtained at different depths of anodic oxide. In Fig. 2d the profiles corresponding to Hf and O are presented and for each electrolyte dilution the concentrations are given as measured on the surface (0 nm depth) and after removal of 2, 6 and 12 nm of oxide. Observing the uniformity of Hf/O ratio in-depth and across different electrolyte dilutions it may be concluded that the composition of HfO_2 was invariable. However, the O/Hf ratio is larger than 2 indicating the presence of electrolyte species inside the anodic oxide. High resolution XPS peaks of Hf 4f are presented in Fig. 2e as measured on oxides grown in different concentrations. Lower PB dilutions resulted in clearly distinguishable HfO_2 peaks as observed by comparing experimental data and the 5/2 and 7/2 database peaks. However, in case of 1 M electrolyte, a clear chemical shift is observed for the Hf 4f doublet. This is attributed to the presence of Hf-O-P bonds as indicated by the corresponding reference. In Fig. 2f the depth profiles of P and Na can be followed for different PBs. The Na amount decreased with the depth and increased with the electrolyte concentration, reaching 1.5 at.% for 1 M PB. The P amount showed a similar trend, its surface concentration reaching 7.5 at.% for 1 M PB. Based on these observations, it can be inferred that overall the concentration of phosphates decreased with the depth independent on PBs. The highest phosphates concertation was confirmed for the 1 M PB but no electrolyte species could be found deep inside HfO_2. This could be linked to the formation of Hf-O-P bonds at and close to the surface that are impeding electrolyte incorporation for thicker oxides. Bonding of phosphate species with Hf may suggest a strong electrolyte incorporation effect with direct influences on CF localization within the oxide and electric performance of memristors.

Fig. 3 is a summary of the electrical behavior of memristors in the line with ReRAMs memory characteristics and device performance (lifetime and loses). The switching behavior of memristors grown in different PB dilutions are shown in Fig. 3a, b, and c where both current-voltage (*I-U*) and conductance-voltage (*G-U*) sweeps are presented. A slightly asymmetric bipolar switching is detected, in agreement with Zaffora et *al* [25]. In addition, the switching is successfully done up to 5 V in each case, the conductance is in the nS range and current compliance was never reached. Although very small current compliances (down to nA) were tried to be employed during the measurements, the memristive switching always fell into voltage limitation, pointing out that only few CFs may be formed. It is likely that the conductance appears in a low range due to the insulating properties of Hf, but still the difference between ON and OFF states is noticeable [27]. This difference often expressed as the ON/OFF ratio is a general and important property of memristive devices. In this study its value is higher than 10, and comparable to previous findings [24,38]. The consistency of the ON/OFF ratio values can be recognized within the context of retention and endurance measurements as well.

The retention or reading test is probing the long-term memory of ON or OFF states by successive readings for a high number of cycles. The applied voltage is kept at low levels (0.02 V) for ensuring that the current state is not changed/switched. Generally, the retention attained at

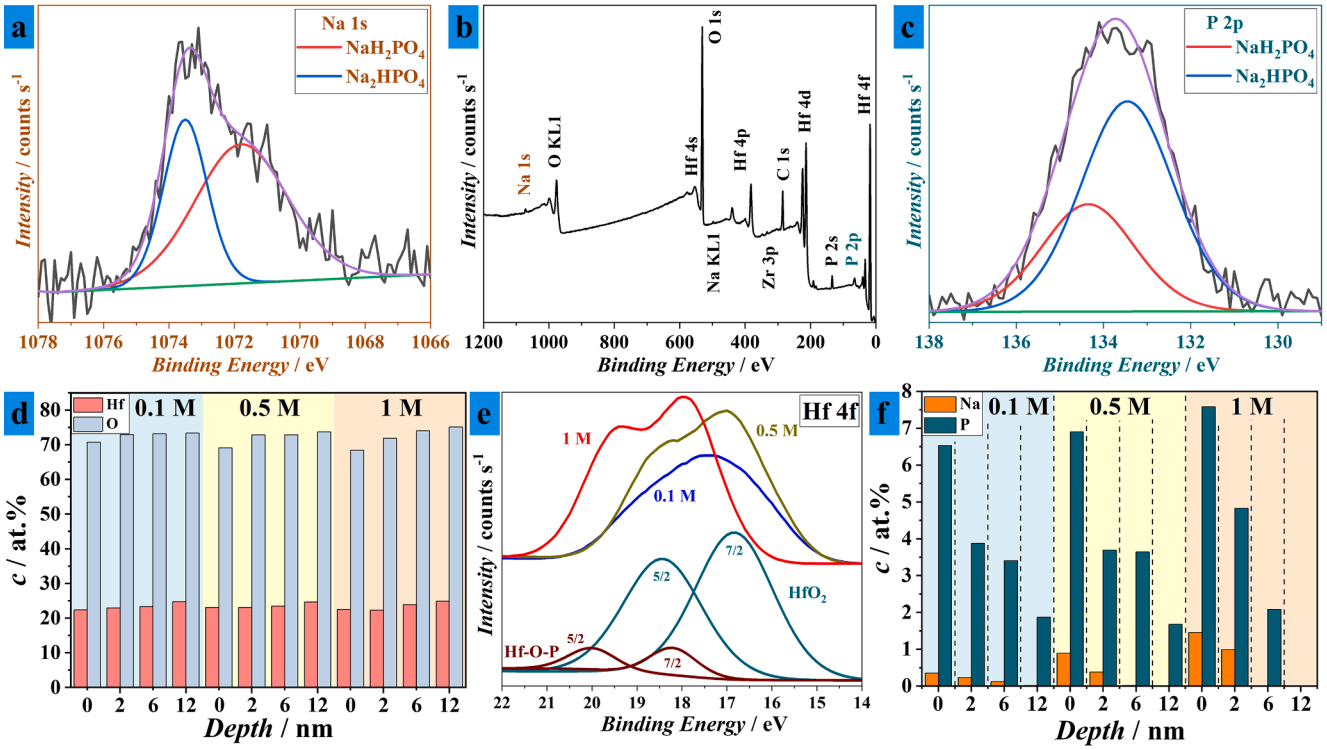

Fig. 2. Chemical analysis of anodic Hf memristors: Surface XPS survey (b) with high resolution analysis of Na (a), P (c) and Hf (e) peaks and quantitative analysis by depth profiling of Hf and O (d) and electrolyte species (f).

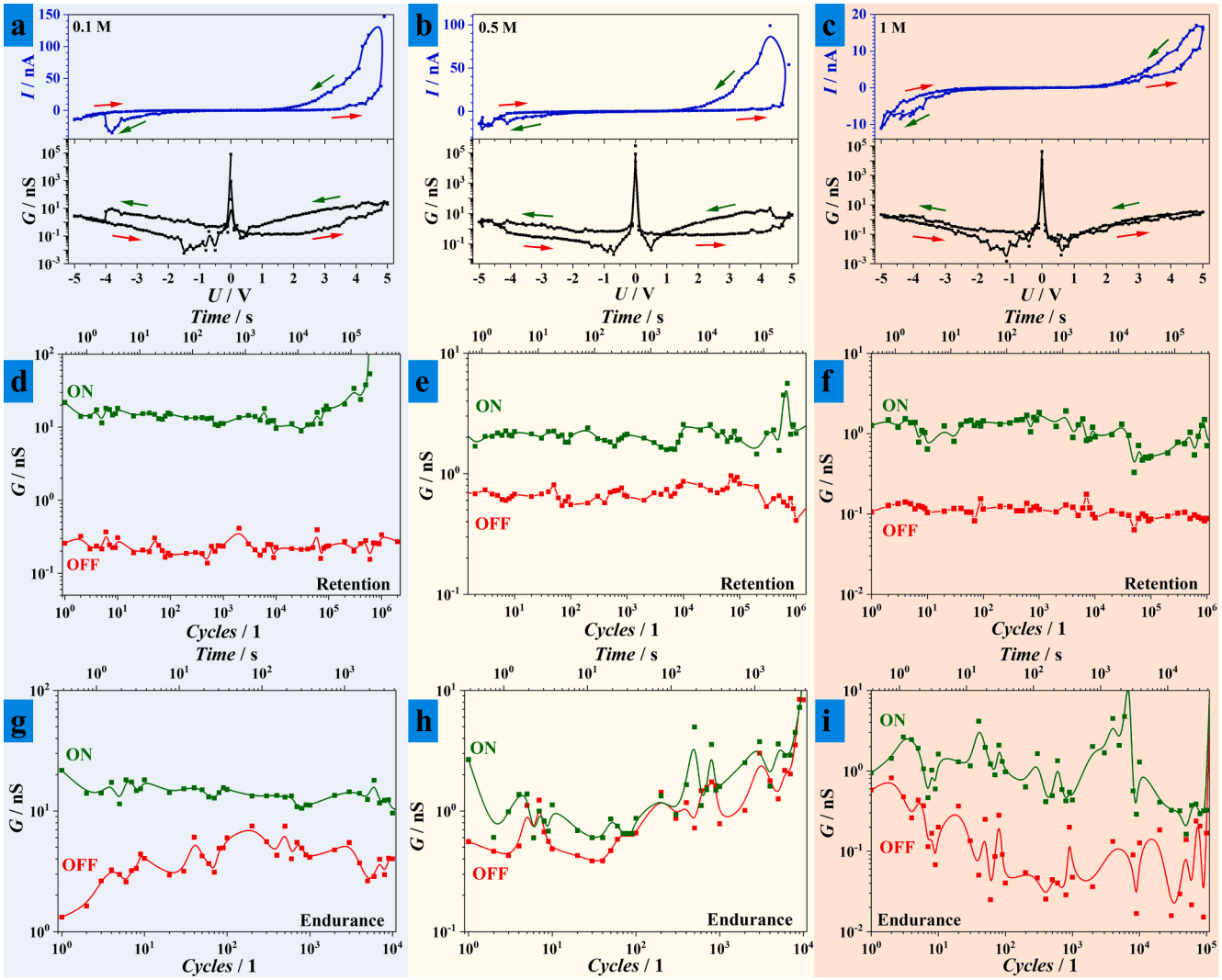

Fig. 3. Memristive characteristics for anodic Hf memristors grown in different concentration of phosphate buffer electrolytes: Memristive switching characteristics (a-c), retention (d-f) and endurance (g-i) testing.

least 10^6 cycles for all anodic memristors investigated here, and their OFF state remained rather constant during testing (see Fig. 3d-f). The memristors fabricated in 0.1 M PB increased their conductivity slightly before the 10^6 cycle. This may be related to the CFs formation which is mainly based on the oxygen vacancies movement in case of the HfO_2 memristors [39]. The size and shape of the CF is established during filament formation defining the performance of the memristive device [33,39]. The conductive filament is known to be thermodynamically unstable and prone to thermal disturbances, thus a sudden diffusion of oxygen vacancies into the CF-ruptured region may occur during the retention period. In this way, the increase of oxygen vacancies concentration within the CF region and whole memory cell may cause a strengthening of the CF or reconnection of the broken filament leading to an increase of the ON state conductance and retention failure [39].

The endurance, often described as the writing procedure, provides the maximum possible number of switching cycles between OFF and ON states. The results for the different concentrations of PB varied. Devices formed in 1 M PB achieved fatigue up to 10^5 cycles, whereas for 0.1 M PB and 0.5 M PB, the devices failed earlier at 10^4 cycles. The conductance of OFF and ON states fluctuated with increasing cycles for the middle concentration of PB. However, the conductance for ON state increased with the cycle number and the conductance of the OFF state decreased for 1 M and 0.1 M PB. This may be directly linked to the CF formation. The bonding between Hf and P (*via* O) determined for the most concentrated PB may benefit the constant positioning of CF resulting in a spatial pining. The formation of such stronger CF leads to a longer life time and lower fluctuations of the device.

Until now, the influence of electrolyte selection on the behavior of Hf anodic memristors was not reported. However, Ti anodic memristors fabricated using different sodium and phosphoric electrolytes were reported as insensitive to incorporated electrolyte species. Still, the incorporation of phosphorus may inhibit the crystallization of TiO_2, thus forming amorphous oxide allowing lower cycle-to-cycle variability of memristors [40]. Similarities may be found in the present work, but the electrolyte incorporation into HfO_2 did not completely disturb the crystalline nature of the oxide in order to improve variability, as in the case of Ti. This is suggested by the rather noisy endurance curves observed during the use of PB with high concentrations (Fig. 3h and i). Other studies on Hf, Nb and Ta anodic memristors are mostly based on anodization in borate buffer electrolyte due to clearly identified multi -level switching, which is not very clear for PB formed devices (even though is not impossible). [6,9,25] However, the retention and endurance of PB formed devices presented in the current study are superior to those corresponding to borate electrolytes. Beside the chemical advantages of using PB, the incorporation the phosphorous species inside the active oxide layer has promoted the electrical properties of anodic memristors, especially from the endurance and retention point of view.

Thermo-electrical measurements were performed by heating the

anodic memristors formed at room temperature up to 80 °C for assessing the maximum operating temperature of memristors. This is relevant in particular to ReRAMs since most motherboards function only up to temperatures in the range of 80 °C [39]. The significant effect of oxygen and moisture on the switching features was previously discussed and mild heat treatments may influence the electric behaviour [41]. In Fig. 4 a summary of the thermo-electrical measurements is provided. The conductance increased to S range due to the heat treatment for all PBs as seen in parts a-c of the figure. Generally, the ON state of memristors became highly conductive (10^{-1}S). The OFF state conductance increased at least three orders of magnitude and the difference between the ON and OFF states was higher in case of 0.1 M and 1 M, as compared to the same memristors operating at room temperature (Fig. 4a and c). As it can be seen in Fig. 4b, the middle concentration (0.5 M) provides irreproducible devices with hardly distinguishable conductance levels (ON/OFF ratio), whereas the 1 M PB shows a maximum value of the ratio at 50 °C. For that reason, the endurance and retention testing (Fig. 4d, f) was performed at 50 °C for 1 M devices resulting in cycling up to 10^5 cycles before failure. The values of the ON state remained stable after each cycle, but the OFF values slightly increased. This is also observable in Fig. 4e where exemplary *I-U* curves are presented as recorded after different cycles. In summary, the memristors anodized in 0.1 M and 1 M PB have significantly improved their electrical performance while operating at temperatures around 50 °C. With this regard, even at temperatures up to 80 °C, the devices did not prematurely fail during retention or endurance testing. When the memristors were cooled down to room temperature, their ON/OFF ratios and state conductivities also dropped back to their initial values measured immediately after formation. Therefore, the heat treatment applied in this work allows identifying the best device operating temperatures and cannot be used as a post-fabrication treatment aimed to increase device stability. The improvement achieved by memristive switching at higher temperature should be related to redox reactions based on moisture incorporation providing additional O vacancies inside the oxide and affecting its memristive switching [41]. Therefore, the anodic HfO_2 memristors are simple and cheap candidates for ReRAMs in electronic systems operating at temperatures up to 80 °C.

4. Conclusions

The incorporation of electrolyte species in anodic Hf memristors was demonstrated for the first time. Phosphate species have a significant impact on the CFs formation inside the insulating HfO_2 layer, as demonstrated by chemical analysis of oxides grown in different PB concentrations. The use of 1 M PB was found to promote formation of Hf-O-P compounds that likely form a barrier impeding further phosphate incorporation into the bulk of the memristor. Endurance, retention and memory characteristics of Hf memristors are analysed and their improved properties and simplified fabrication is concluded by comparison with literature reports.

Impact statement

Understanding the phosphate concentration role in growth of anodic hafnia memristors allows a proper electrolyte selection for applications. Phosphates incorporation enhance memristive characteristics, while no additional fabrication requirements are necessary.

CRediT authorship contribution statement

Ivana Zrinski: Data curation, Formal analysis, Investigation, Validation, Visualization, Writing - original draft, Writing - review & editing. **Cezarina Cela Mardare:** Data curation, Methodology, Validation, Visualization, Writing - original draft. **Luiza-Izabela Jinga:** Formal analysis, Resources, Validation, Writing - original draft. **Jan Philipp Kollender:** Data curation, Methodology, Validation, Visualization, Writing - original draft. **Gabriel Socol:** Formal analysis, Resources, Validation, Writing - original draft. **Achim Walter Hassel:** Data curation, Methodology, Validation, Visualization, Writing - original draft. **Andrei Ionut Mardare:** Conceptualization, Data curation, Formal analysis, Funding acquisition, Investigation, Methodology, Project administration, Resources, Software, Supervision, Validation,

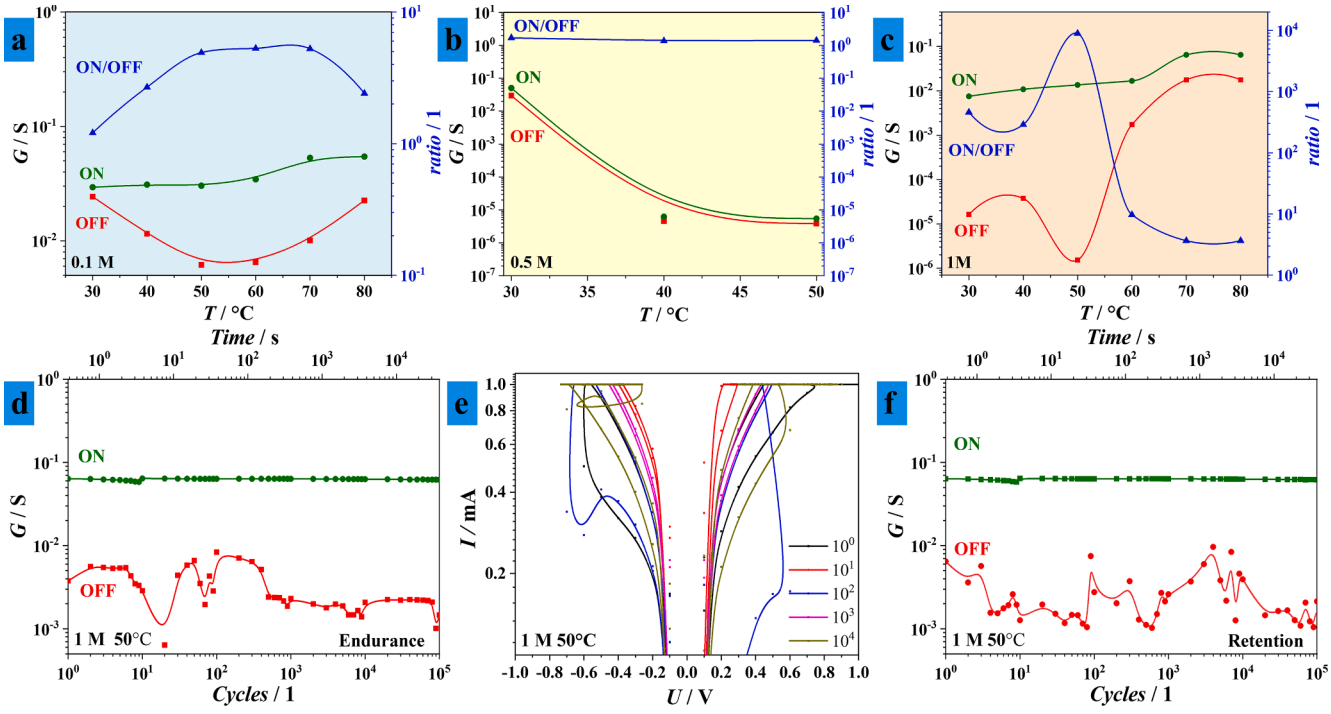

Fig. 4. Mild heat treatment effects on memristive behaviour: Temperature dependent ON and OFF states for different electrolyte concentrations (a-c), endurance and retention at 50 °C for the highest electrolyte concentration (d, f) and exemplary *I-U* curves during cycling (e).

Visualization, Writing - original draft, Writing - review & editing.

Declaration of Competing Interest

The authors declare that they have no known competing financial interests or personal relationships that could have appeared to influence the work reported in this paper.

Acknowledgements

The financial support from the Austrian Science Fund (FWF): P 32847-N and the experimental support (FIB and TEM) of Günter Hesser and Peter Oberhumer from the Zentrum für Oberflächen- und Nanoanalytik (ZONA) at Johannes Kepler University Linz are gratefully acknowledged.

References

[1] J.J. Yang, M.D. Pickett, X. Li, D.A.A. Ohlberg, D.R. Stewart, R.S. Williams, Memristive switching mechanism for metal/oxide/metal nanodevices, Nat. Nanotechnol. 3 (2008) 429–433, https://doi.org/10.1038/nnano.2008.160.
[2] K.M. Kim, B.J. Choi, C.S. Hwang, Localized switching mechanism in resistive switching of atomic-layer-deposited TiO2 thin films, Appl. Phys. Lett. 90 (2007) 242906, https://doi.org/10.1063/1.2748312.
[3] S. Dirkmann, J. Kaiser, C. Wenger, T. Mussenbrock, Filament growth and resistive switching in hafnium oxide memristive devices, ACS Appl. Mater. Interfaces 10 (2018) 14857–14868, https://doi.org/10.1021/acsami.7b19836.
[4] T. Ishibe, Y. Maeda, T. Terada, N. Naruse, Y. Mera, E. Kobayashi, Y. Nakamura, Resistive switching memory performance in oxide hetero-nanocrystals with well-controlled interfaces, Sci. Technol. Adv. Mater. 21 (2020) 195–204, https://doi.org/10.1080/14686996.2020.1736948.
[5] S. Almeida, B. Aguirre, N. Marquez, J. McClure, D. Zubia, Resistive switching of SnO2 thin films on glass substrates, Integr. Ferroelectr. 126 (2011) 117–124, https://doi.org/10.1080/10584587.2011.575015.
[6] A. Zaffora, F. Di Quarto, H. Habazaki, I. Valov, M. Santamaria, Electrochemically prepared oxides for resistive switching memories, Faraday Discuss. 213 (2019) 165–181, https://doi.org/10.1039/c8fd00112j.
[7] T.V. Kundozerova, G.B. Stefanovich, A.M. Grishin, Binary anodic oxides for memristor-type nonvolatile memory, Phys. Status Solidi Curr. Top. Solid State Phys. 9 (2012) 1699–1701, https://doi.org/10.1002/pssc.201100625.
[8] T.V. Kundozerova, A.M. Grishin, G.B. Stefanovich, A.A. Velichko, Anodic Nb 2O 5 nonvolatile RRAM, IEEE Trans. Electron Dev. 59 (2012) 1144–1148, https://doi.org/10.1109/TED.2011.2182515.
[9] A. Zaffora, D.Y. Cho, K.S. Lee, F. Di Quarto, R. Waser, M. Santamaria, I. Valov, Electrochemical tantalum oxide for resistive switching memories, Adv. Mater. 29 (2017) 1–6, https://doi.org/10.1002/adma.201703357.
[10] V. Aglieri, A. Zaffora, G. Lullo, M. Santamaria, F. Di Franco, U. Lo Cicero, M. Mosca, R. Macaluso, Resistive switching in microscale anodic titanium dioxide-based memristors, Superlattices Microstruct. 113 (2018) 135–142, https://doi.org/10.1016/j.spmi.2017.10.031.
[11] A.I. Mardare, A. Ludwig, A. Savan, A.W. Hassel, Properties of anodic oxides grown on a hafnium-tantalum-titanium thin film library, Sci. Technol. Adv. Mater. 15 (2014), https://doi.org/10.1088/1468-6996/15/1/015006.
[12] D. Ielmini, Resistive switching memories based on metal oxides: mechanisms, reliability and scaling, Semicond. Sci. Technol. 31 (2016) 1–25, https://doi.org/10.1088/0268-1242/31/6/063002.
[13] S. Abdul Hadi, K.M. Humood, M. Abi Jaoude, H. Abunahla, H.F. Al Shehhi, B. Mohammad, Bipolar Cu/HfO2/p++ Si memristors by sol-gel spin coating method and their application to environmental sensing, Sci. Rep. 9 (2019) 1–15, https://doi.org/10.1038/s41598-019-46443-x.
[14] G.W. Burr, R.M. Shelby, A. Sebastian, S. Kim, S. Kim, S. Sidler, K. Virwani, M. Ishii, P. Narayanan, A. Fumarola, L.L. Sanches, I. Boybat, M. Le Gallo, K. Moon, J. Woo, H. Hwang, Y. Leblebici, Neuromorphic computing using non-volatile memory, Adv. Phys. X 2 (2017) 89–124, https://doi.org/10.1080/23746149.2016.1259585.
[15] J.F. Vanhumbeeck, J. Proost, Current understanding of ti anodisation: functional, morphological, chemical and mechanical aspects, Corros. Rev. 27 (2009) 117–204, https://doi.org/10.1515/CORRREV.2009.27.3.117.
[16] J.A. Bardwell, P. Schmuki, G.I. Sproule, D. Landheer, D.F. Mitchell, Physical and electrical characterization of thin anodic oxides on Si(100), J. Electrochem. Soc. 142 (1995) 3933–3940, https://doi.org/10.1149/1.2048437.
[17] H. Efeoglu, S. Güllülü, T. Karacali, Resistive switching of reactive sputtered TiO2 based memristor in crossbar geometry, Appl. Surf. Sci. 350 (2015) 10–13, https://doi.org/10.1016/j.apsusc.2015.03.088.
[18] M. Zhang, S. Long, Y. Li, Q. Liu, H. Lv, E. Miranda, J. Suñé, M. Liu, Analysis on the filament structure evolution in reset transition of Cu/HfO2/Pt RRAM device, Nanoscale Res. Lett. 11 (2016), https://doi.org/10.1186/s11671-016-1484-8.
[19] M.J. Wang, S. Gao, F. Zeng, C. Song, F. Pan, Unipolar resistive switching with forming-free and self-rectifying effects in Cu/HfO2/n-Si devices, AIP Adv. 6 (2016), https://doi.org/10.1063/1.4941839.
[20] G.I. Tselikov, A. EmelyanovV, I.M. Antropov, V.A. Demin, P.K. Kashkarov, Effect of TiOx/TiO2 layer thickness on the properties of the pulsed laser deposited memristive device, Phys. Status Solidi Curr. Top. Solid State Phys. 12 (2015) 229–232, https://doi.org/10.1002/pssc.201400123.
[21] R. Macaluso, M. Mosca, V. Costanza, A. D'Angelo, G. Lullo, F. Caruso, C. Calì, F. Di Franco, M. Santamaria, F. Di Quarto, Resistive switching behaviour in ZnO and VO2 memristors grown by pulsed laser deposition, Electron. Lett. 50 (2014) 262–263, https://doi.org/10.1049/el.2013.3175.
[22] H. Abunahla, B. Mohammad, M.A. Jaoude, M. Al-Qutayri, Novel hafnium oxide memristor device: Switching behaviour and size effect, Proc. - IEEE Int. Symp. Circuits Syst. (2017) 7–10, https://doi.org/10.1109/ISCAS.2017.8050791.
[23] L. Assaud, K. Pitzschel, M.K.S. Barr, M. Petit, G. Monier, M. Hanbücken, L. Santinacci, Atomic layer deposition of HfO 2 for integration into three-dimensional metal–insulator–metal devices, Appl. Phys. A Mater. Sci. Process. 123 (2017) 1–7, https://doi.org/10.1007/s00339-017-1379-2.
[24] L. Wu, H. Liu, J. Li, S. Wang, X. Wang, A multi-level memristor based on Al-doped HfO2 thin film, Nanoscale Res. Lett. 14 (2019), https://doi.org/10.1186/s11671-019-3015-x.
[25] A. Zaffora, F. Di Franco, F. Di Quarto, R. Macaluso, M. Mosca, H. Habazaki, M. Santamaria, The effect of Nb incorporation on the electronic properties of anodic HfO 2, ECS J. Solid State Sci. Technol. 6 (2017) N25–N31, https://doi.org/10.1149/2.0121704jss.
[26] A.R. Teren, P. Ehrhart, R. Waser, J.Q. He, C.L. Jia, M. Schumacher, J. Lindner, P. K. Baumann, T.J. Leedham, S.R. Rushworth, A.C. Jones, Comparison of hafnium precursors for the MOCVD of HfO 2 for gate dielectric applications, Integr. Ferroelectr. 57 (2003) 1163–1173, https://doi.org/10.1080/714040772.
[27] J.H. Choi, Y. Mao, J.P. Chang, Development of hafnium based high-k materials - a review, Mater. Sci. Eng. R Reports. 72 (2011) 97–136, https://doi.org/10.1016/j.mser.2010.12.001.
[28] Sodium phosphate, Cold Spring Harb. Protoc. 2006 (2006) pdb.rec8303. DOI: 10.1101/pdb.rec8303.
[29] D. Briggs, X-ray photoelectron spectroscopy (XPS), Handb. Adhes. Second Ed. (2005) 621–622, https://doi.org/10.1002/0470014229.ch22.
[30] M.M. Lohrengel, A Review Journal, Mater. Sci. 12 (1993) 243–294, https://doi.org/10.1016/0927-796X(94)90011-6.
[31] M. Schie, M.P. Müller, M. Salinga, R. Waser, R.A. De Souza, Ion migration in crystalline and amorphous HfOX, J. Chem. Phys. 146 (2017), https://doi.org/10.1063/1.4977453.
[32] E.M. Patrito, V.A. Macagno, C. Quimicas, Characterization of hafnium anodic oxide films: an ac impedance investigation, Electrochim. Acta. 40 (1995) 809–815, https://doi.org/10.1016/0013-4686(95)00003-W.
[33] W. Xue, Y. Li, G. Liu, Z. Wang, W. Xiao, K. Jiang, Z. Zhong, S. Gao, J. Ding, X. Miao, X.H. Xu, R.W. Li, Controllable and Stable quantized conductance states in a Pt/HfOx/ITO memristor, Adv. Electron. Mater. 6 (2020) 1–9, https://doi.org/10.1002/aelm.201901055.
[34] H.A. Abd El-Rahman, M.M. Abou-Romia, Anodization of hafnium in phosphoric acid solutions, J. Appl. Electrochem. 20 (1990) 39–44, https://doi.org/10.1007/BF01012469.
[35] M.T. Thomas, Preparation and properties of sputtered hafnium and anodic HfO[sub 2] films, J. Electrochem. Soc. 117 (1970) 396, https://doi.org/10.1149/1.2407522.
[36] A.I. Mardare, C.M. Siket, A. Gavrilović-Wohlmuther, C. Kleber, S. Bauer, A. W. Hassel, Anodization behavior of glassy metallic hafnium thin films, J. Electrochem. Soc. 162 (2015) E30–E36, https://doi.org/10.1149/2.0021504jes.
[37] K. Thomsen, R. Gani, P. Rasmussen, Synthesis and analysis of processes with electrolyte mixtures, Comput. Chem. Eng. 19 (1995) 27–32, https://doi.org/10.1016/0098-1354(95)87010-5.
[38] H. García, L.A. Domínguez, H. Castán, S. Dueñas, Control of the set and reset voltage polarity in anti-series and anti-parallel resistive switching structures, Microelectron. Eng. 216 (2019) 111083, https://doi.org/10.1016/j.mee.2019.111083.
[39] G.S. Kim, T.H. Park, H.J. Kim, T.J. Ha, W.Y. Park, S.G. Kim, C.S. Hwang, Investigation of the retention performance of an ultra-thin HfO2 resistance switching layer in an integrated memory device, J. Appl. Phys. 124 (2018) 024102, https://doi.org/10.1063/1.5033967.
[40] S. Chen, S. Noori, M.A. Villena, Y. Shi, T. Han, Y. Zuo, M.P. Pedeferri, D. Strukov, M. Lanza, M.V. Diamanti, Memristive electronic synapses made by anodic oxidation, Chem. Mater. 31 (2019) 8394–8401, https://doi.org/10.1021/acs.chemmater.9b02245.
[41] M. Lübben, S. Wiefels, R. Waser, I. Valov, Processes and effects of oxygen and moisture in resistively switching TaOx and HfOx, Adv. Electron. Mater. 4 (2018) 1–11, https://doi.org/10.1002/aelm.201700458.